

## ***The Solidification Behavior of an Alloy 625/718 Variant\****

**M. J. Cieslak**

**Sandia National Laboratories  
Albuquerque, New Mexico 87185**

### **Abstract**

The solidification behavior of Custom Age 625 PLUS® is examined using an integrated analytical approach. Like its predecessors, Alloys 625 and 718, the solidification behavior of this new alloy is dominated by the presence and segregation of Nb, which gives rise to a  $\gamma$ /Laves terminal solidification constituent.

\*This work performed at Sandia National Laboratories supported by the U.S. Dept. of Energy under contract number DE-AC04-76DP00789.

Superalloys 718, 625 and Various Derivatives  
Edited by Edward A. Loria  
The Minerals, Metals & Materials Society, 1991

## **Introduction**

Since their commercial introduction over two decades ago, Alloys 625 and 718 have been among the most successfully applied nickel base superalloys in engineering applications. Because of continually expanding service requirements, such as higher temperature exposure or more aggressive corrosive environments, variants of these two alloys have been developed which are now beginning to see industrial applications. As these alloys will necessarily experience solidification processing (arc melting, casting, welding), an understanding of the microstructural development associated with solidification is imperative. In this paper, we will describe the solidification behavior of the new wrought alloy, Carpenter Custom Age 625 PLUS®, and compare it with previously reported data on Alloys 625 and 718.

## **Experimental**

The experimental techniques used to examine the alloys discussed in this work include differential thermal analysis (DTA), optical metallography, electron microprobe analysis, and scanning and transmission electron microscopy. Autogenous (no filler metal added) gas tungsten arc fusion welds were also examined. The compositions of the heat of Custom Age 625 PLUS® examined in this study is listed in Table 1.

DTA experiments were performed on a Netsch Thermal Analyzer STA 429. The specimens were heated and cooled through the melting/solidification temperature range at the rate of 20°C/min. Samples weighed less than 5 grams and all tests were run under a flowing helium atmosphere. To calibrate the system, nickel specimens were tested and were found to melt within 2°C of the established literature value. Reactions were identified as deviations from the local baseline. The liquidus temperature was identified as the peak of the on-heating endotherm.

Metallographic techniques involved optical and scanning electron microscopy. Microanalysis was performed using a Cameca MBX microprobe and a JEOL 2000FX analytical electron microscope. Individual phases were identified using selected area electron diffraction. AEM/EDS techniques were used to qualitatively determine phase chemistry.

## **Results**

Figure 1 shows the DTA thermograms obtained during testing of Custom Age 625 PLUS®. Melting initiates as the solidus is exceeded at 1257°C and terminates at the liquidus of 1356°C. There appears only a single event on the melting thermogram indicating simple single phase melting. The on-cooling portion of the thermogram (exothermic reactions) shows markedly different behavior. Solid nucleates at 1330°C (26°C of undercooling) and continues to grow at the expense of the liquid phase until a terminal solidification event occurs at 1126°C.

Analysis of solidification microstructures and alloying element segregation was performed on weld metal as it was felt that the structures and segregation patterns would be much better preserved in weld metal cooling from the solidus at rates in excess of 100°C/s as compared to fractions of a °C/s in the DTA tests.

Figure 2a shows the fusion zone microstructure observed in a weldability test specimen from Custom Age 625 PLUS®. A small volume fraction of interdendritic constituent is observed and this constituent is also intimately associated with an induced hot crack. Shown in greater detail in Figure 2b, the eutectic-like nature of this constituent becomes apparent. Figure 3a is a TEM thin foil micrograph taken from a sample prepared from the fusion zone of this alloy and shows the distribution of Laves phase. The matrix is austenitic and the minor constituent (arrows) had its electron diffraction pattern indexed as a hexagonal Laves phase. In addition to these two phases, a closer examination of the austenitic matrix immediately adjacent to the Laves (Fig. 3b) revealed a very fine, but dense, precipitation of  $\gamma'$ . Figure 4 shows AEM EDS spectra taken from the Laves phase and the matrix  $\gamma$ . Note the high Nb concentration in the Laves.

Figure 5 shows the pattern of elemental segregation associated with the solidification of Custom Age 625 PLUS®. Dendrite core regions, the first volumes to solidify, are regions of high Ni, Fe, and Cr concentration. Nb, Ti, and Mo all segregate to interdendritic volumes, those regions where solidification terminates.

## **Discussion**

The solidification behavior of the variant of Alloys 625 and 718 retains an important feature from the original alloys. All of the newer alloys also contain from  $\approx 3$  wt.% to  $> 5$  wt.% Nb. It is the presence of Nb in these alloys which dominates the solidification behavior. As can be seen in Fig. 5, the extent of Nb segregation is far greater than that of any other alloying element examined. In fact, it is the presence of Nb which ultimately gives rise to eutectic-like solidification constituents involving Laves phase (i.e a  $\gamma$ /Laves constituent).

That Nb is required in this alloy family for the  $\gamma$ /Laves constituent to appear in the solidification microstructure has been shown conclusively in a study by Cieslak et al.[1] of Alloy 625. In that study alloys which were chemically identical to Alloy 625, but which were Nb-free, did not form Laves-containing solidification constituents. In that same study, it was found that minor elements could have substantial impact on the solidification structure observed in Alloy 625. Si, for example promoted the formation of an increased amount of the Laves solidification constituent, consistent with observations made by Wlodek [2] in the solid state in superalloys. An  $M_6C$  carbide-containing constituent was also noted at high Si concentration. It is extremely interesting to note that while no  $Ni_2Nb$  Laves phase exists, a ternary Laves phase of the form  $Ni_3SiNb_2$  has been identified by Bardos et al. [3]. C promoted the formation of an  $M(Nb)C$  carbide type eutectic-like constituent at the expense of the Laves constituent. In fact, the presence of C at a concentration of 0.038 wt.% resulted in the effective elimination of the Laves solidification constituent in Alloy 625.

Custom Age 625 PLUS® appears to solidify in a manner not much different from a low carbon Alloy 625. That is, the only constituent observed in the solidified microstructure of Custom Age 625 PLUS® is the Laves-containing constituent. The carbon content is too low to be effective in promoting a carbide solidification product. This behavior is also consistent with observations made in Incoloy 909 [4]. That alloy contains very little carbon, typically  $< 0.005$  wt.%, and its solidification microstructure is free of carbide solidification products. In comparison to a low-Si (0.03 wt.%), low Fe (2.30 wt.%) Alloy 625, the volume fraction of the Laves solidification constituent in Custom Age 625 PLUS® is higher [5], likely the result of the higher Fe content and the addition of Ti, a Laves phase forming element, in this new alloy.

The high yield strength ( $> 120$  ksi) of Custom Age 625 PLUS® invites closer comparison with Alloy 718. In general, Alloy 718 is not commercially available as an ultra-low carbon alloy. Typically, Alloy 718 contains 0.04 wt.% C. At this level of carbon and with a higher Nb concentration ( $> 5$  wt.%), Alloy 718 contains both a Laves phase and a carbide (MC) solidification product [6-8]. This higher Nb concentration, in addition to a large ( $\approx 18$  wt.%) Fe concentration, promotes a volume fraction of terminal solidification product, especially the Laves constituent, (often between 5 and 10 volume percent [6]) that is far in excess of what is seen in Custom Age 625 PLUS® ( $\approx 1$  volume percent). For comparison purposes, the solidification constituents found in Alloys 625, 718, and 909 are listed in Table 2 along with their approximate formation temperatures.

## **Conclusions**

The solidification behavior of Custom Age 625 PLUS® is dominated by the presence and segregation behavior of Nb. In a manner analogous to Alloys 625 and 718, solidification terminates with the formation of a Nb-rich  $\gamma$ /Laves eutectic-like constituent. The low C content of this alloy precludes the formation of eutectic-like carbides.

### References

1. M. J. Cieslak, T. J. Headley, T. Kollie, and A. D. Romig, Jr., *Metallurgical Transactions A*, 19A, No. 9, 1988, pp. 2319-2331.
2. S. T. Wlodek, *Trans. Am. Soc. Met.*, 56 (1963), pp. 287-303.
3. D. I. Bardos, K. P. Gupta, and P. A. Beck, *Trans. TMS-AIME*, 221 (1961), p. 1087.
4. M. J. Cieslak, T. J. Headley, G. A. Knorovsky, A. D. Romig, Jr., T. Kollie, *Metallurgical Transactions A*, 21(A), No. 2, 1990, pp. 479-488.
5. M. J. Cieslak, T. J. Headley, R. B. Frank, *Welding Journal*, Vol. 68, No. 12, 1989, pp. 473-s - 482-s.
6. G. A. Knorovsky, M. J. Cieslak, T. J. Headley, A. D. Romig, Jr., and W. F. Hammetter, *Metallurgical Transactions A*, 20(A), No. 10, 1989, pp. 2149-2158.
7. M. J. Cieslak, G. A. Knorovsky, T. J. Headley, and A. D. Romig, Jr., *Metallurgical Transactions A*, 17A, No. 12, 1986, pp. 2107-2116.
8. M. J. Cieslak, G. A. Knorovsky, T. J. Headley, A. D. Romig, Jr., *Superalloy 718 Metallurgy and Applications*, E. A. Loria, ed., TMS publication, 1989, pp. 59-68.

**Table 1.**

**Alloy Composition (wt.%)**

<b>Element</b>	<b>Custom Age 625 PLUS</b>
<b>C</b>	<b>0.009</b>
<b>Mn</b>	<b>0.08</b>
<b>Si</b>	<b>0.03</b>
<b>P</b>	<b>0.007</b>
<b>S</b>	<b>0.002</b>
<b>Cr</b>	<b>21.03</b>
<b>Ni</b>	<b>60.87</b>
<b>Mo</b>	<b>7.96</b>
<b>Nb</b>	<b>3.39</b>
<b>Ti</b>	<b>1.31</b>
<b>Al</b>	<b>0.18</b>
<b>B</b>	<b>0.0035</b>
<b>Fe</b>	<b>5.18</b>

**Table 2.**

**Comparative Terminal Solidification Constituents\***

<b>Alloy</b>	<b>Constituent (Temperature)</b>
<b>625 (0.009 wt.% C, 0.03 wt.% Si)</b>	$\gamma$ /Laves ( $\approx 1150^{\circ}\text{C}$ )
<b>625 (0.038 wt.% C, 0.03 wt.% Si)</b>	$\gamma$ /MC ( $\approx 1250^{\circ}\text{C}$ )
<b>625 (0.008 wt.% C, 0.38 wt.% Si)</b>	$\gamma$ /Laves ( $\approx 1150^{\circ}\text{C}$ ), $\gamma$ /M <sub>6</sub> C ( $\approx 1200^{\circ}\text{C}$ )
<b>625 (0.035 wt.% C, 0.46 wt.% Si)</b>	$\gamma$ /MC ( $\approx 1230^{\circ}\text{C}$ ), $\gamma$ /Laves ( $\approx 1160^{\circ}\text{C}$ )
<b>718 (0.04 wt.% C, 0.21 wt.% Si)</b>	$\gamma$ /MC ( $\approx 1260^{\circ}\text{C}$ ), $\gamma$ /Laves ( $\approx 1185^{\circ}\text{C}$ )
<b>909 (0.003 wt.% C, 0.48 wt.% Si)</b>	$\gamma$ /Laves ( $\approx 1200^{\circ}\text{C}$ )

\* Temperatures all determined from DTA tests at 20°C/s cooling rate from Refs. [1,4,6]

CARPENTER CUSTOM AGE 625 PLUS

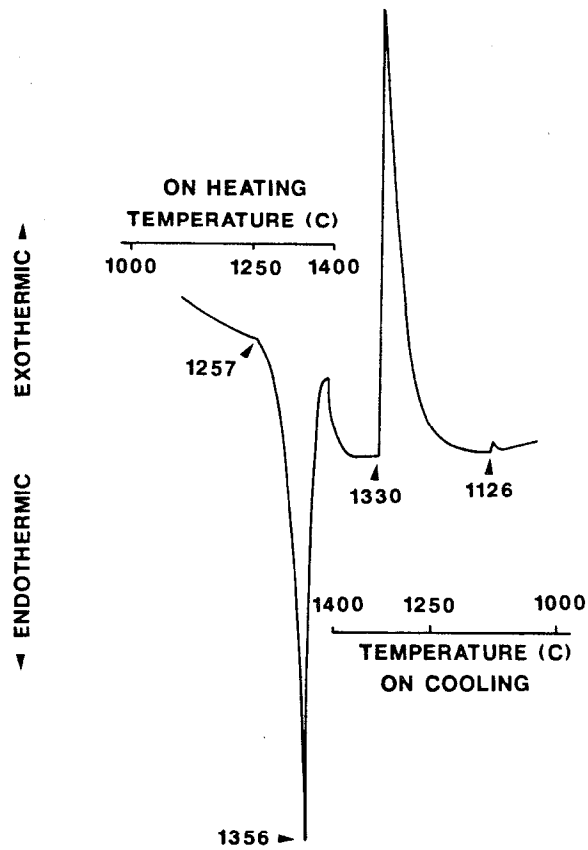


Figure 1. DTA thermogram (20°C/min) of Custom Age 625 PLUS™.

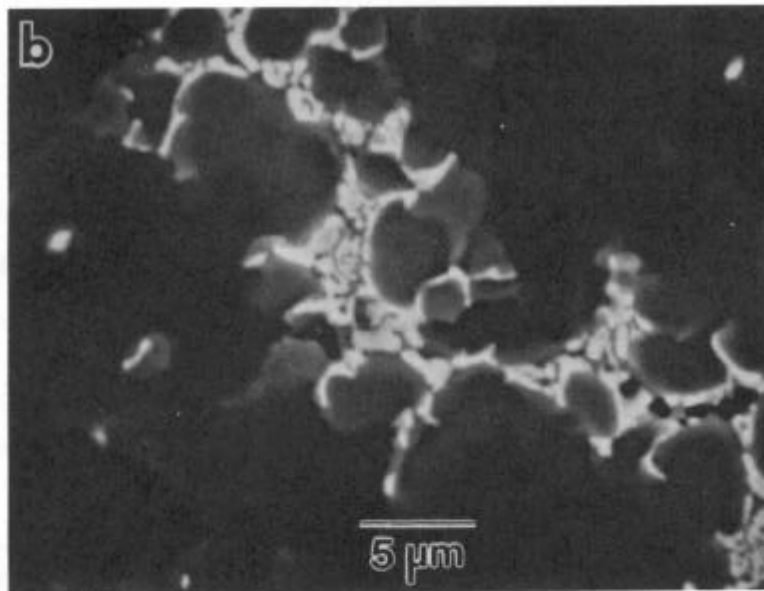
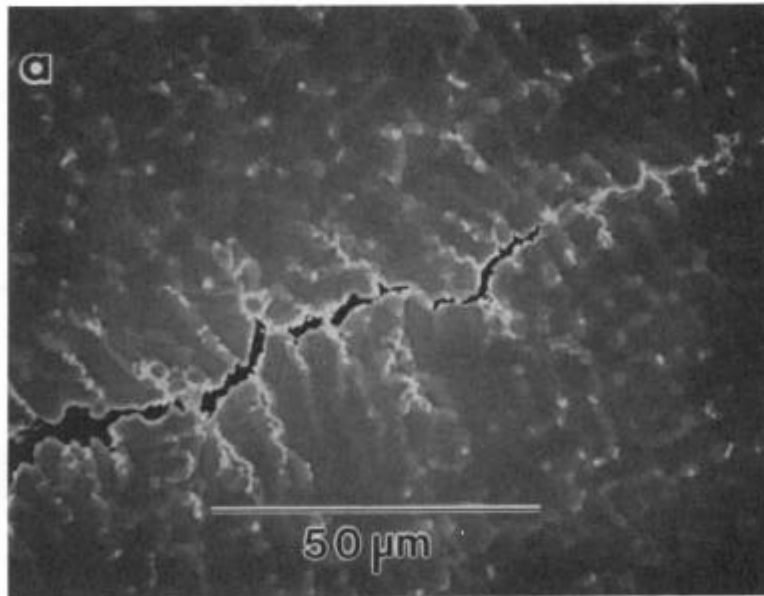


Figure 2. (a) SEM micrograph of an induced fusion zone hot crack in GTA weld metal of Alloy 625 PLUS® showing interdendritic constituent associated with the crack. (b) Higher magnification image showing eutectic-like morphology of this constituent.

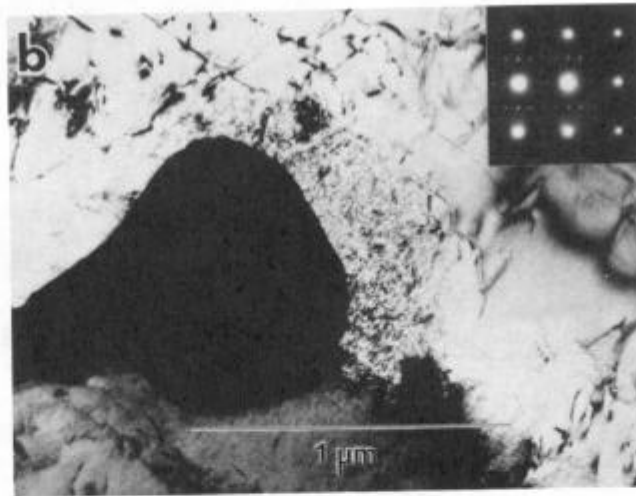
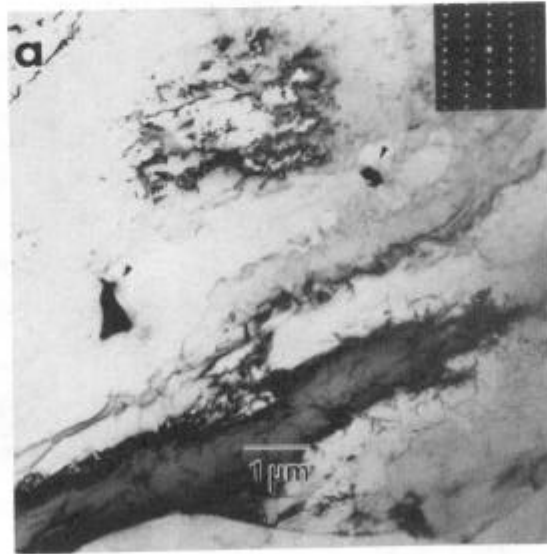


Figure 3. (a) TEM thin foil micrograph showing Laves distribution in GTA weld metal. Shown is the electron diffraction pattern from the  $[11\bar{2}0]$  zone from the Laves. (b) Higher magnification TEM thin foil micrograph showing distribution of  $\gamma'$  (speckled appearance) adjacent to Laves (dark phase) in GTA weld metal. Electron diffraction pattern shows  $[100]$  zone from the  $\gamma$  matrix (large bright spots) and diffraction spots (fainter, smaller spots) from the family of  $[100]$ ,  $[010]$ , and  $[001]$  zones in  $\gamma'$ .



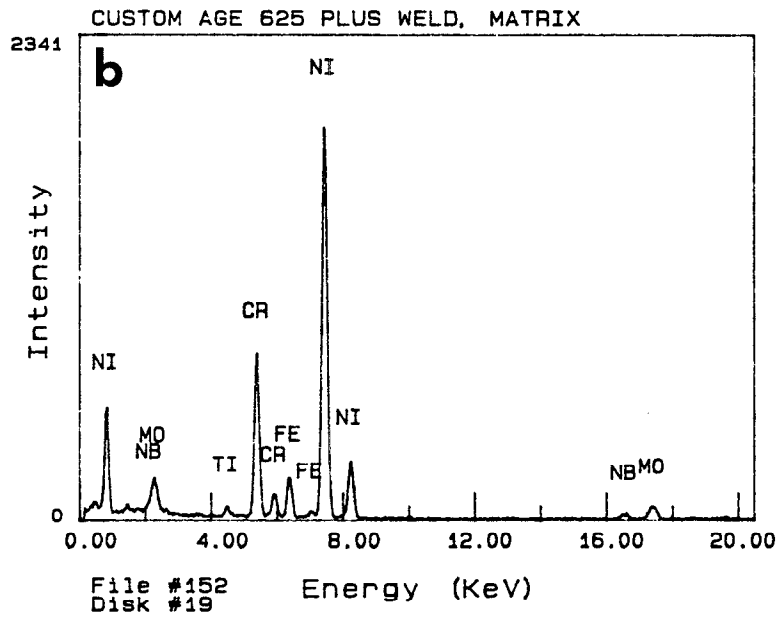
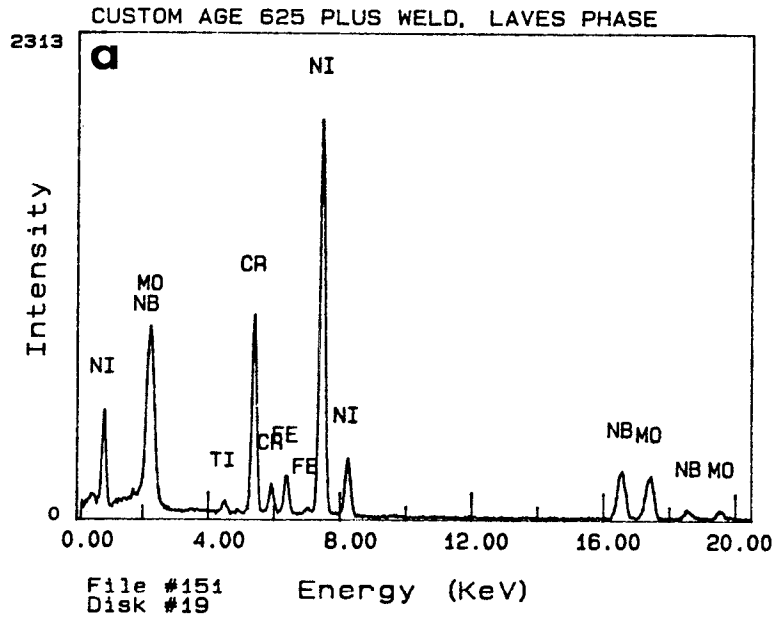


Figure 4. (a) AEM EDS spectra taken from Laves phase in the fusion zone of GTA weld metal. (b) AEM EDS spectra taken from the  $\gamma$  matrix in the fusion zone of GTA weld metal.

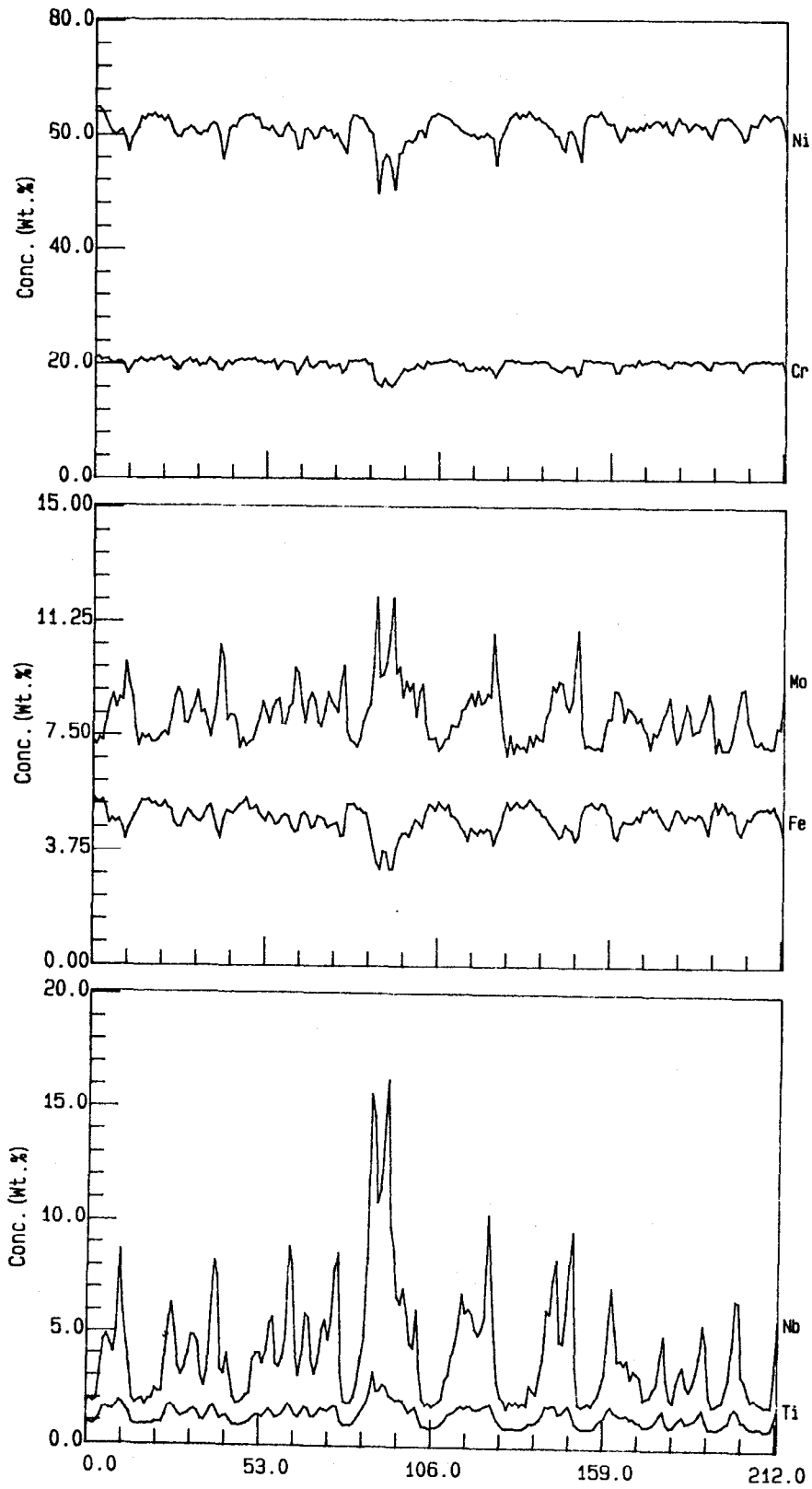


Figure 5. Electron microprobe trace across GTA weld metal. Regions of high Ni, Fe, and Cr are dendrite cores. Regions of high Nb, Ti, and Mo are interdendritic regions. Position units in  $\mu\text{m}$ . Trace crosses constituent associated with a hot crack at  $\sim 85 \mu\text{m}$  position.